CI&CEQ
Chemical Industry & Chemical Engineering Quarterly

Available on line at
Association of the Chemical Engineers of Serbia *AChE*
www.ache.org.rs/CICEQ

Chem. Ind. Chem. Eng. Q. 21 (2) 319–330 (2015) CI&CEQ

LAWRENCE KOECH[1]
RAY EVERSON[2]
HEIN NEOMAGUS[2]
HILARY RUTTO[1]

[1]Department of Chemical Engineering, Vanderbijlpark Campus, Vaal University Of Technology, Vanderbijlpark, South Africa
[2]Department of Chemical and Minerals Engineering, Potchefstroom Campus, North West University, Potchefstroom, South Africa

SCIENTIFIC PAPER

UDC 66.094.522.091.8:662.613.1

DOI 10.2298/CICEQ140423032K

DISSOLUTION KINETICS OF SOUTH AFRICAN COAL FLY ASH AND THE DEVELOPMENT OF A SEMI-EMPIRICAL MODEL TO PREDICT DISSOLUTION

Article Highlights

- Dissolution kinetics of fly ash using adipic acid at constant pH was investigated
- A semi-empirical model was developed to predict dissolution of fly ash
- The sorbent before and after dissolution was characterized XRF, FTIR, BET surface area and SEM

Abstract

Wet flue gas desulphurization (FGD) is a crucial technology which can be used to abate the emission of sulphur dioxide in coal power plants. The dissolution of coal fly ash in adipic acid is investigated by varying acid concentration (0.05--0.15 M), particle size (45-150 μm), pH (5.5-7.0), temperature (318-363 K) and solid-to-liquid ratio (5-15 wt.%) over a period of 60 min which is a crucial step in wet (FGD). Characterization of the sorbent was done using X-ray fluorescence (XRF), X-ray diffraction (XRD), Furrier transform infrared (FTIR), scanning electron microscope (SEM) and Branauer-Emmett-Teller (BET) surface area. BET surface area results showed an increase in the specific surface area and SEM observation indicated a porous structure was formed after dissolution. The experimental data was analyzed using the shrinking core model and the diffusion through the product layer was found to be the rate limiting step. The activation energy for the process was calculated to be 10.64 kJ/mol.

Keywords: flue gas desulphurization, coal fly ash, dissolution, shrinking core model, activation energy.

The increase in the use of coal in thermal power plants has led to an increase in production of waste such as coal fly ash. Coal fly ash is an industrial by-product generated during coal combustion for production of energy. It is collected before flue gas reaches the chimney using either electro-static precipitators, bag filters or cyclones. It is considered hazardous because it contains elements such as boron, vanadium, chromium and arsenic which are harmful to the environment [1,2]. Fly ash is largely used in concrete as cement replacement and making geo-polymers. However, most of the fly ash produced is disposed in ash ponds or landfills [3,4].

Correspondence: H. Rutto, Department of Chemical Engineering, Vanderbijlpark Campus, Vaal University Of Technology, Private Bag X021, Vanderbijlpark, 1900 South Africa.
E-mail: hilaryr@vut.ac.za
Paper received: 23 April, 2014
Paper revised: 14 August, 2014
Paper accepted: 9 September, 2014

Because fly ash is a waste material, it is economical to be used as a partial substitute or as a reagent in flue gas desulphurization (FGD). It is mainly composed of SiO_2, Al_2O_3, CaO and Fe_2O_3 [5]. It can therefore be utilized in FGD processes as a supplement to act as a source of Ca^{2+}, Al^{3+} and Si^{4+} which can improve the total SO_2 removal efficiency in both wet and dry flue gas desulphurization systems [6]. Studies have shown that sorbents prepared from fly ash exhibit improved reactivity towards SO_2 and also improved sorbent utilization. The amorphous silica in fly ash reacts with hydrated lime to form calcium silicate hydrates in the presence of water (pozzolanic reaction). The calcium silicate hydrates attach to each other forming large particles with more porous structure which leads to an increase in sorbent surface area and improved pore volume [7-9].

Fly ash dissolution is dependent on its chemical composition and the dissolution process variables such as temperature, particle size, acid concentration,

pH and solid-to-liquid ratio. A study by Kashiwakura [10] on the dissolution of solenoid from coal fly ash particles found out that it is dependent on the pH and acid concentration. Brouwers and Van [11] did a theoretical study on the dissolution of pulverized powder coal fly ash. A shrinking core model was developed for the outer and inner region to explain the behavior of the reaction rate constant as the solid changes. It was reported that the reactivity of fly ash corresponds to the silica content and the outer region is less reactive than the inner region. Pietersen [12] observed a significant increase in dissolution rate of fly ash with increase in the reactant pH (NaOH solution) and also increase in the ambient temperature. A study by Tanaka and Fujii [13] showed that fly ash dissolution is greatly affected by the presence of Si^{4+} and Al^{3+}. The presence of these ions in solution increases with increase in dissolution period and is accelerated with increased stirring speed. Si^{4+} and Al^{3+} are reagents for pozzolanic reaction which takes place in presence of water and leads to formation of products with high surface area.

This study looks into the possibility of using fly ash in wet flue gas desulphurization with a focus on its dissolution kinetics in adipic acid using a pH stat apparatus. It is an improvement to the previous work [14] on dissolution of fly ash for wet FDG process. The extend of dissolution of fly ash is determined by analyzing the amount calcium ions leached into solution which is the most active component during sorbent-SO_2 reaction. Using the experimental data to fit into the shrinking model, a semi-empirical model to describe the dissolution of calcium ions from fly ash was developed. The sorbent before and after dissolution was characterized using BET surface area, XRD and SEM.

MATERIALS AND EXPERIMENTAL METHODS

Materials

Coal fly ash was obtained from a coal-fired thermal power plant. XRF results showed that the chemical composition of the studied fly ash in wt.% consisted of: 49.71 SiO_2, 32.12 Al_2O_3, 10.52 CaO, 3.89 Fe_2O_3, 1.89 TiO_2, 0.15 H_2O and 1.92 loss on ignition. Coal fly ash was crushed using a ball mill and sieved to different particle sizes using shaking screen sieves. Adipic acid and Calcium ion standards for the AAS were supplied by CJ Labs.

Experimental

A given amount of coal fly ash was added to the reactor vessel containing a solution. The temperature, solid-to-liquid ratio, particle size and acid concentration were varied at constant stiring speed of 200 rpm. This was done using a temperature controlled magnetic stirrer. The pH of the reaction mixture was determined using a pH electrode dipped into the solution and connected to a pH controller. When the pH exceeds the set value, the pump is activated to add acid to the reaction vessel and lowers the pH value to the set point.

The sample was then removed, filtered and prepared for analysis of calcium ions using atomic absorption spectrophotometer (AAS). Three calcium standard solutions (1, 5 and 10 ppm) were first prepared from the calcium ion standards for the AAS (1000 ppm). The standard solution was used to calibrate the AAS machine before analyzing the samples. The AAS machine atomizes the samples in the flame, through which radiation of a chosen wavelength (using a hollow cathode lamp) is sent. The amount of absorbed radiation is a quantitative measure for the concentration of the element to be analyzed. The gas mixture of acetylene and nitrous-oxide was used in the AAS instrument.

The dissolution fraction was calculated as:

$$X = \frac{\text{Calcium ions in solution}}{\text{Total amount of calciuim ions in the original sample}}$$

Characterization techniques

Qualitative and quantitative analysis of the studied fly ash before and after dissolution was done using XRD. A back loading preparation method was used for XRD analysis. Two samples were scanned after addition of 20% Si for qualitative determination of amorphous content. It was analyzed with a PANalytical Empyrean diffractometer with PIXcel detector and fixed with Fe filtered CoKα radiation. X'pert Highscore Plus software was used to identify the phases present in the samples.

The functional groups present in the samples were determined using FTIR analysis. The analysis determined using a Perkin Elmer spectrum (400FT--IR/FT-NIR) machine equipped with a universal attenuated total reflectance (ATR) accessory. There was no sample preparation required for the instrument. The samples were scanned at a range of 4000 to 650 cm^{-1}.

The surface area analysis was conducted using Micrometrics 2020 porosity analyser. The samples were degassed at 150 °C under vacuum condition for 24 h using nitrogen gas. The specific surface area was determined using the Brunauer-Emmett-Teller (BET) method. The microporous volume and area were obtained using the Barrett-Joyner-Halenda (BJH) procedure.

The morphological structure of the samples at different dissolution periods was studied using scanning electron microscopy (SEM). The samples were sprinkled on an adhesive carbon tape and were metallized using gold before the analysis. The images of the samples were recorded at various magnifications.

RESULTS AND DISCUSSION

Mechanism for dissolution of fly ash in adipic acid

Coal fly ash mainly consists of SiO_2, Al_2O_3, CaO Fe_2O_3 and TiO_2. These are chemical components that will be affected as dissolution takes place. The mechanism for dissolution of SiO_2, Al_2O_3, CaO Fe_2O_3 and TiO_2 in adipic acid is therefore shown in Eqs. (2)-(6).

Adipic acid dissociates into solution to form adipate ions:

$$C_6H_{10}O_{4(aq)} \rightarrow C_6H_8O_{4(aq)}^{2-} + 2H_{(aq)}^{+} \quad (1)$$

The dissolution of SiO_2, Al_2O_3, CaO, Fe_2O_3 and TiO_2 is by adipate complexation to form their respective adipate complexes [10]:

$$SiO_{2(s)} + 2C_6H_8O_{4(aq)}^{2-} + 4H_{(aq)}^{+} \rightarrow \rightarrow Si(C_6H_8O_4)_{2(aq)} + 2H_2O_{(l)} \quad (2)$$

$$Al_2O_{3(s)} + 3C_6H_8O_{4(aq)}^{2-} + 6H_{(aq)}^{+} \rightarrow \rightarrow Al_2(C_6H_8O_4)_{3(aq)} + 3H_2O_{(l)} \quad (3)$$

$$TiO_{2(s)} + 2C_6H_8O_{4(aq)}^{2-} + 4H_{(aq)}^{+} \rightarrow \rightarrow Ti(C_6H_8O_4)_{2(aq)} + 2H_2O_{(l)} \quad (4)$$

$$CaO_{(s)} + C_6H_8O_{4(aq)}^{2-} + H_2O_{(l)} \rightarrow \rightarrow Ca(C_6H_8O_4)_{(aq)} + 2OH_{(aq)}^{-} \quad (5)$$

$$Fe_2O_{3(s)} + 3C_6H_8O_{4(aq)}^{2-} + 3H_2O_{(l)} \rightarrow \rightarrow Fe_2(C_6H_8O_4)_{3(aq)} + 6OH_{(aq)}^{-} \quad (6)$$

Dissociation of silicon, aluminium, titanium, iron and calcium adipate in the bulk will occur due to supersaturation [15]. This leads to formation of silicon, aluminium, titanium, iron and calcium ions in solution with adipate ions [10].

$$Si(C_6H_8O_4)_{2(aq)} \rightleftharpoons Si_{(aq)}^{4+} + 2C_6H_8O_{4(aq)}^{2-} \quad (7)$$

$$Al_2(C_6H_8O_4)_{3(aq)} \rightleftharpoons 2Al_{(aq)}^{3+} + 3C_6H_8O_{4(aq)}^{2-} \quad (8)$$

$$Ti(C_6H_8O_4)_{2(aq)} \rightleftharpoons Ti_{(aq)}^{4+} + 2C_6H_8O_{4(aq)}^{2-} \quad (9)$$

$$CaC_6H_8O_{4(aq)} \rightleftharpoons Ca_{(aq)}^{2+} + C_6H_8O_{4(aq)}^{2-} \quad (10)$$

$$Fe_2(C_6H_8O_4)_{3(aq)} \rightleftharpoons 2Fe_{(aq)}^{3+} + 3C_6H_8O_{4(aq)}^{2-} \quad (11)$$

The presence of CaO in the coal fly ash is important because Ca^{2+} is the most reactive ion during chemo-sorption reaction in flue gas desulphurization. Apart from dissolution by adipate complexation (Eq. (5)), hydrogen complexation can also cause CaO dissolution releasing calcium ions into solution [16].

CaO dissolution by hydrogen complexation:

$$CaO_{(s)} + H_{(aq)}^{+} \rightarrow Ca_{(aq)}^{2+} + OH_{(aq)}^{-} \quad (12)$$

Calcium ions from supersaturation (Eq. (10)) can be utilized more in pozzolanic reaction with fly ash being the source of silica and alumina to form aluminosilicate complex compounds [17].

Pozzolanic reaction:

$$Ca_{(aq)}^{2+} + 2SiO_{2(s)} + Al_2O_{3(s)} + OH_{(aq)}^{-} \rightarrow \rightarrow CaAl_2Si_2O_8 \cdot H_2O_{(s)} \quad (13)$$

Calcium aluminosilicate hydrate is formed from the pozzolanic reaction which increases the surface area of the sorbent and hence improve the rate of SO_2 absorption in flue gas desulphurization.

XRD analysis

XRD analysis was used to determine the structural changes of coal fly ash after dissolution has taken place. The results are represented in Figure 1. The diffraction peaks exhibited by raw fly ash shows that it is mainly composed of quartz (SiO_2)-Q, mullite ($Al_6Si_2O_{13}$)-M and silicon (Si)-S. The silicon and quartz peaks diminish after 30 min and more after 60 min dissolution period. This shows that dissolution had an effect on these compounds and they were leached into solution.

A new diffraction peak appears at $2\theta = 33°$ in the sorbents after dissolution. This can be identified as anorthite ($CaAl_2Si_2O_8$). Dissolution of fly ash leads to Si^{4+} and Al^{3+} being leached out of the amorphous aluminosilicate of fly ash. Leaching of these ions (Si^{4+} and Al^{3+}) increases with prolonged dissolution. A pozzolanic reaction occurs and anorthite is formed in the sorbents after dissolution [18]. Pozzolanic reaction leads to the formation of sorbents with high surface area which can eventually improve SO_2 absorption capacity during flue gas desulphurization.

BET specific surface area

The nitrogen adsorption desorption isotherm plot for fly ash before and after dissolution is illustrated in Figure 2a. The figure clearly shows that the sorbents have an adsorption isotherm of type II according the IUPAC classification [19]. This indicates that porosity of fly ash sorbent after dissolution was in the meso-

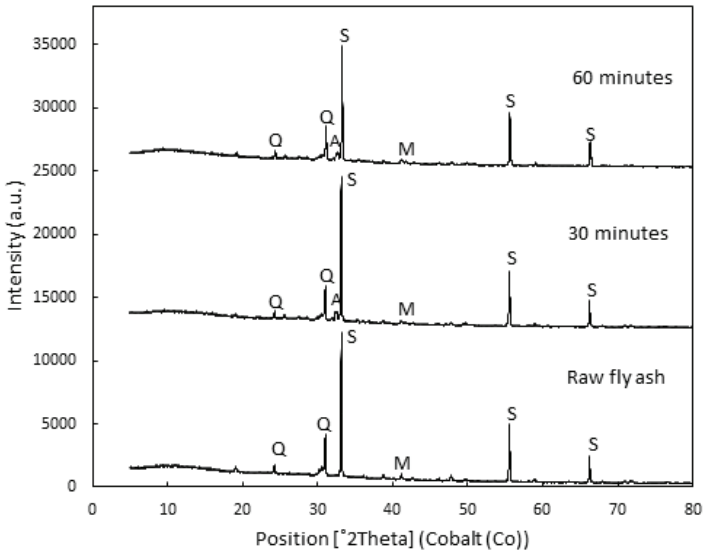

Figure 1. XRD patterns for raw fly ash and sorbents after 30 and 60 min dissolution period (S - silicon, Q - quartz, M - mullite, A - anorthite).

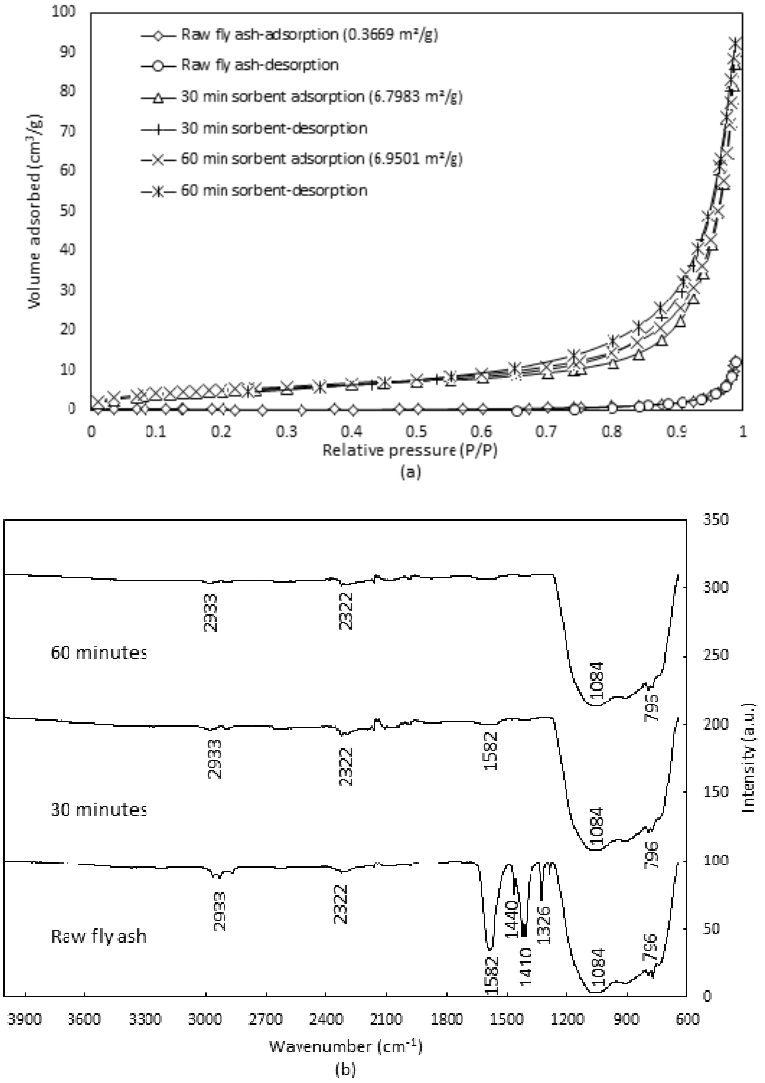

Figure 2. Adsorption-desorption isotherm plot (a) and FTIR spectra (b) for fly ash at different dissolution periods.

pore range. The mesopore range is an effective zone for sulphation reaction between calcium ions and SO_2 during flue gas desulphurization [7].

The specific surface area increases significantly with prolonged dissolution period (from 0.3669 to 6.9501 m^2/g). The increase in surface area is attributed to the products of pozzolanic reaction which yields complex aluminosilicate compounds which are responsible for increased specific surface area in the sorbent [20]. The increase in the specific surface area shows that the formation of calcium aluminosilcate complex continued to change the structure of the particles into a more porous form [8].

FTIR analysis

The chemical heterogeneity of fly ash at different dissolution periods is shown in Figure 2b. From the diagram, the samples exhibited overlapping absorption bands between 1200 and 900 cm^{-1}. These overlapping bands indicate the presence of quartz and mullite in the samples [21] and it is also due to the asymmetrical stretching of amorphous aluminosilicate formed by the reaction of extracted Si^{4+} and Al^{3+} ions. The series of bands representing quartz appear at 1084 and 796 cm^{-1}.

The bands appearing at 1410, 1440 and 1582 cm^{-1} are assigned to the asymmetrical stretching vibration of CaO band [22]. The depleted peaks of CaO band is due to the effect of dissolution after which CaO goes into solution. This is excellent agreement with the results from XRD analysis.

Surface morphology

Figure 3 shows the surface morphology of fly ash samples at different dissolution periods. Raw fly ash mainly consists of particles that are rounded and spherical in shape with smooth surfaces. The smooth surface in the fly ash is due to aluminosilicate particles that are formed as a result of transformation of mineral particles during coal combustion [23].

The sorbents after exposure to dissolution had their surfaces relatively rough and porous compared to raw fly ash. The sorbent also exhibited deformation of the smooth surfaces after dissolution; this was observed in the sorbent after 60 min dissolution period. This indicates that the aluminosilicate compounds in particles of fly ash were extracted into solution [24]. The agglomerated particles in the sorbent after dissolution is attributed to the formation of calcium aluminosilicate compounds. This is a product of pozzolanic reaction during dissolution as shown in Eq. (13). The porous structure combined with agglomerated particles results in an increase in the specific surface area of the sorbents which can improve the SO_2 absorption capacity in flue gas desulphurization [25].

Effect of reaction variables

Effect of solid-to-liquid ratio

The effect of solid-to-liquid ratio on dissolution of fly ash in adipic acid was done in the range of 5-15 wt.%. The temperature, pH, particle size and acid concentration were kept constant at 60 °C, 5.5, 45 μm and 0.1 M, respectively. The experimental results are represented in Figure 4a. It is evident that the conversion of calcium ions into solution is higher at lower solid-to-liquid ratio compared to higher solid-to-liquid ratio within the same dissolution period. This is attributed to the decrease in the fluid reactant per unit weight of the solid as solid-to-liquid ratio increases.

Effect of acid concentration

To investigate the effect of acid concentration on dissolution of fly ash, different experiments were per-

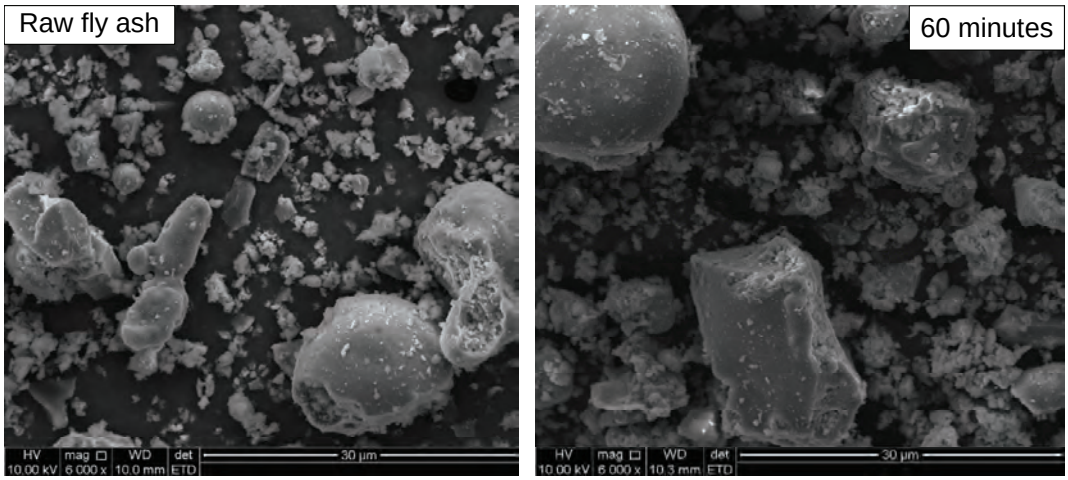

Figure 3. SEM micrographs for raw fly ash and sorbent after 60 min dissolution period.

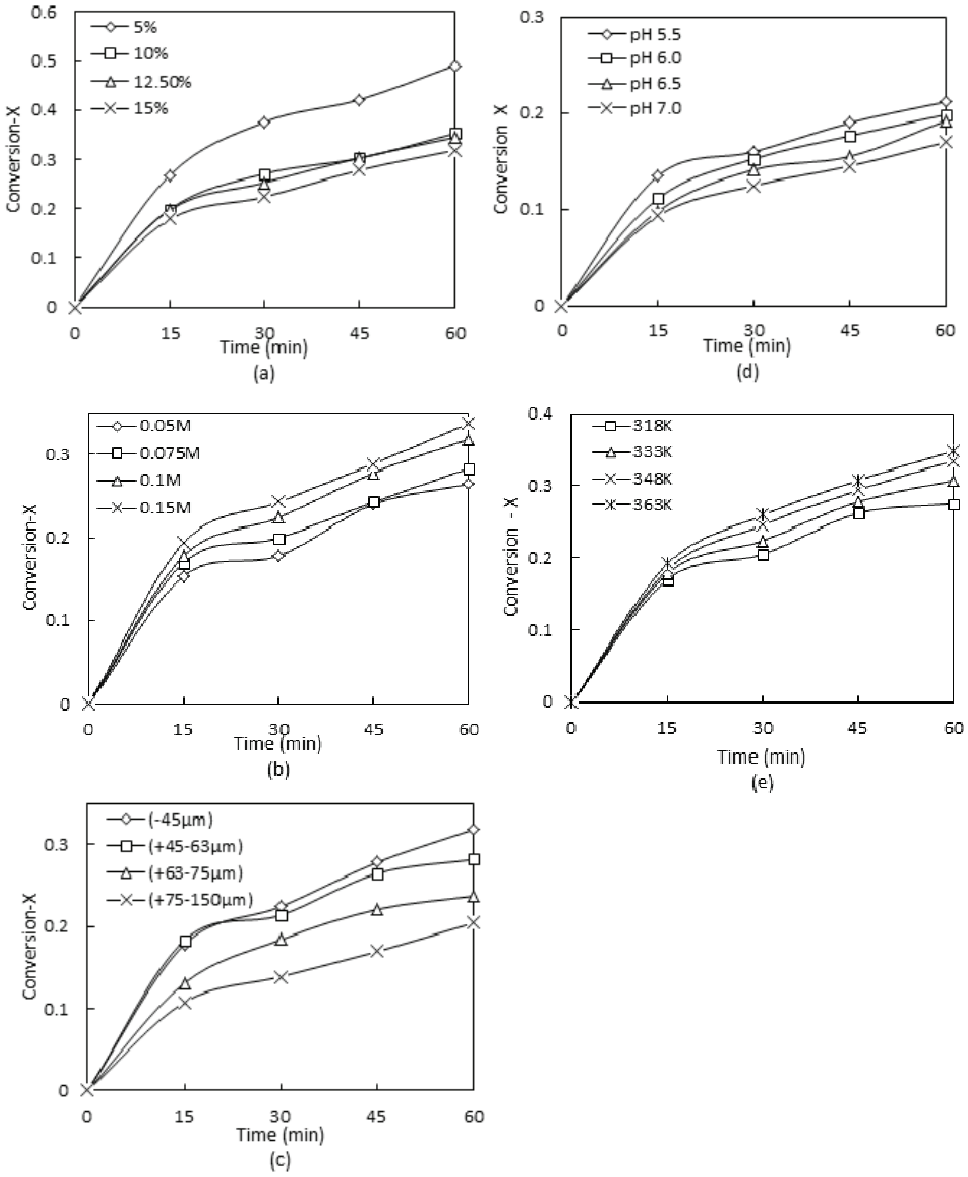

Figure 4. Effect of solid-to-liquid ratio (a), acid concentration (b), particle size (c), pH (d) and temperature (e) on the dissolution of fly ash.

formed at a range of 0.05-0.15 M adipic acid. The temperature, pH, particle size and solid-to-liquid ratio were kept constant at 60 °C, 5.5, 45 µm and 10 wt.%, respectively. Figure 4b shows the experimental results and it is clear that the conversion of fly ash increases with increase in acid concentration. Increase in acid concentration leads to an increase in H^+ activity in the liquid film therefore enhancing reaction on the solid surface.

Effect of particle size

Four different size fractions were used to investigate the effect of particle size on the dissolution rate of coal fly ash. The average size fractions used were from 45-150 µm. The temperature, pH, solid-to-liquid ratio and acid concentration were kept constant at 60 °C, 5.5, 10 wt.% and 0.1 M, respectively. The experimental results are represented in Figure 4c, which shows that by reducing the particle size of fly ash, it significantly improved the conversion of calcium ions into solution as compared to larger particle size over the same dissolution period. This is because finer particles have higher surface area, thus enhancing dissolution.

Effect of pH

The effect of pH on dissolution of fly ash was studied in the range of 5.5-7.0. The temperature, solid-to-liquid ratio, particle size and acid concentration were kept constant at 60 °C, 10 wt.%, 45 µm and 0.1 M, respectively. Figure 4d represents the experimental results. It is evident that dissolution rate

increases with decrease in pH. This is because the increase in pH causes an increase in the apparent mass transfer coefficient.

Effect of temperature

The effect of temperature on the dissolution rate of fly ash was performed in the range between 318--363 K. The soilid to liquid ratio, pH, particle size and acid concentration were kept constant at 10 wt.%, 5.5, 45 μm and 0.1 M, respectively. The experimental results are depicted in Figure 4e and it can be seen that the conversion of calcium ions is enhanced at higher temperatures than at lower temperatures. High temperatures accelerate the reaction rate because there is an increase in energy which results in more collision between reacting molecules which speeds the reaction.

Dissolution kinetics

The dissolution kinetics of fly ash in adipic acid was studied using the shrinking core model for solid-liquid system. The model considers the reaction of the reactants at the surface of the solid particles which results in both aqueous and solid particles [26]. The unreacted core of the particle reduces in size as the reaction proceeds, with more solids and aqueous products being formed [27]. This model considers the following steps in series:

1. Diffusion of the fluid reactant through the film surrounding the particle to the surface of the solid;
2. Penetration and reaction of the fluid reactant through the layer of ash to the surface of the unreacted core;
3. Fluid-solid surface chemical reaction at the reaction surface.

It is considered that the slowest step is the rate controlling step. From the above reaction steps, a heterogeneous system is considered to be controlled by: film diffusion, product layer diffusion or chemical reaction at the surface of the core of the unreacted particle. [28]. These steps can be integrated and written as follows:

Film diffusion equation,

$$X = \frac{3bk_f C_A}{\rho_B R_o} t = kt \tag{14}$$

Chemical reaction control,

$$1-(1-X)^{\frac{1}{3}} = \frac{bk_s C_A}{\rho_B R_o} t = k_r t \tag{15}$$

Product layer diffusion,

$$1+2(1-X)-3(1-X)^{\frac{2}{3}} = \frac{6bD_e C_A}{\rho_B R_o} t = k_d t \tag{16}$$

The experimental data was fitted into the shrinking core model using Eqs. (15) and (16). The fluid media used for this study is liquid in nature and it is therefore considered that mass transfer across the fluid film will have least effect on the system. Therefore the fluid film diffusion step will not be controlling for this case [29]. The apparent rate constants for chemical reaction and product layer diffusion models were obtained by plotting the left side of Eqs. (15) and (16) with the reaction time. The apparent rate constants from the plots and their correlation coefficients are represented in Table 1.

According to Table 1, the product layer diffusion model had the highest regression coefficients. The linear relationship between

$$1+2(1-X)-3(1-X)^{\frac{2}{3}}$$

and the reaction time is shown in Figure 5a-e for solid-to-liquid ratio (a), acid concentration (b), particle size (c), pH (d) and temperature (e). This therefore shows that the equation for the dissolution kinetics for this process follows the product layer diffusion model and therefore can be written as follows:

$$k_d t = 1+2(1-X)-3(1-X)^{\frac{2}{3}} \tag{17}$$

To include all the reaction parameters, a semi-empirical model can be written as:

$$k_d = K_o C^a \left(\frac{S}{L}\right)^b D^c P^d e^{\left(\frac{-E_a}{RT}\right)} \tag{18}$$

Combining Eqs. (17) and (18) yields:

$$1+2(1-X)-3(1-X)^{\frac{2}{3}} = \\ = K_o C^a \left(\frac{S}{L}\right)^b D^c P^d e^{\left(\frac{-E_a}{RT}\right)} t \tag{19}$$

where C is acid concentration, S/L is solid-to-liquid ratio, D is particle size and P is pH.

The values of the constants a, b, c and d are the reaction orders with respect to each parameter. Their values were obtained by plotting the natural logarithm of the reaction rate constants against natural logarithm of their respective parameter values. Their plots are represented in Figure 6a-d for solid-to-liquid ratio, acid concentration, particle size and pH, respectively.

The Arrhenius plot was used to evaluate the activation energy for the dissolution process. According to the Arrhenius plot (illustrated in Figure 6e), the intercept was found to be 3.5745 and the activation energy evaluated from the slope was 10.64 kJ/mol.

Table 1. Dissolution rate constants and their correlations coefficients

Process variable	Surface chemical reaction $1-(1-X)^{\frac{1}{3}}=k_r t$		Product layer diffusion: $1+2(1-X)-3(1-X)^{\frac{2}{3}}=k_d t$	
	K_r / min^{-1}	R^2	K_d / min^{-1}	R^2
Temperature, K				
318	0.0016	0.8640	0.00049	0.9729
333	0.0019	0.9100	0.00061	0.9961
348	0.0020	0.9096	0.00073	0.9993
363	0.0021	0.9070	0.00080	0.9989
Solid-to-liquid ratio, wt.%				
5	0.0031	0.9129	0.00168	0.9934
10	0.0021	0.8908	0.00080	0.9910
12.5	0.0020	0.8984	0.00077	0.9971
15	0.0019	0.9100	0.00065	0.9961
Concentration, mold m^{-3}				
0.05	0.0015	0.8973	0.00040	0.9804
0.075	0.0016	0.8839	0.00050	0.9837
0.1	0.0019	0.9100	0.00065	0.9961
0.15	0.0020	0.8975	0.00072	0.9935
Particle size, μm				
45	0.0019	0.9100	0.00065	0.9961
63	0.0016	0.8400	0.00050	0.9685
75	0.0014	0.8874	0.00036	0.9861
150	0.0011	0.9175	0.00025	0.9914
pH				
5.5	0.0019	0.8060	0.00065	0.9556
6	0.0018	0.8242	0.00059	0.9698
6.5	0.0017	0.8091	0.00054	0.9519
7	0.0016	0.8342	0.00049	0.9744

The value of the activation energy shows that the dissolution of coal fly ash in adipic acid is a product layer diffusion controlled process. When the activation energy is below 20 kJ/mol, product layer diffusion is usually the rate controlling step [28,30-32].

A semi-empirical model for this process can therefore be written as follows:

$$1+2(1-X)-3(1-X)^{\frac{2}{3}} = 3.5745C^{0.5592}\left(\frac{S}{L}\right)^{-0.8621}D^{-0.8055}P^{-1.196}e^{\left(\frac{-E_a}{RT}\right)}t \quad (20)$$

CONCLUSION

The findings of this study show signigicant effects of the process variables on the dissolution of fly ash in adipic acid. It was found that the dissolution rate increases with increase in temperature and acid concentration, but decreases with increase in particle size, pH, and solid-to-liquid ratio. The pozzolanic reaction resulted in the formation of anorthite as seen in XRD analysis. This also contributed to a significant increase in the specific surface area of sorbent (0.3669 to 6.9501 m^2/g) as observed in the BET surface area analysis. The formation of aggregates and rough surfaces was observed on the surface of the sorbent after dissolution using SEM. The dissolution of fly ash was found to follow the shrinking core model with product layer diffusion model being the rate limiting step. The product layer being reaction products such as anorthite and other compounds. The semi-empirical model describing the dissolution of coal fly ash can be represented as follows:

$$1+2(1-X)-3(1-X)^{\frac{2}{3}} = 3.5745C^{0.5592}\left(\frac{S}{L}\right)^{-0.8621}D^{-0.8055}P^{-1.196}e^{\left(\frac{-E_a}{RT}\right)}t$$

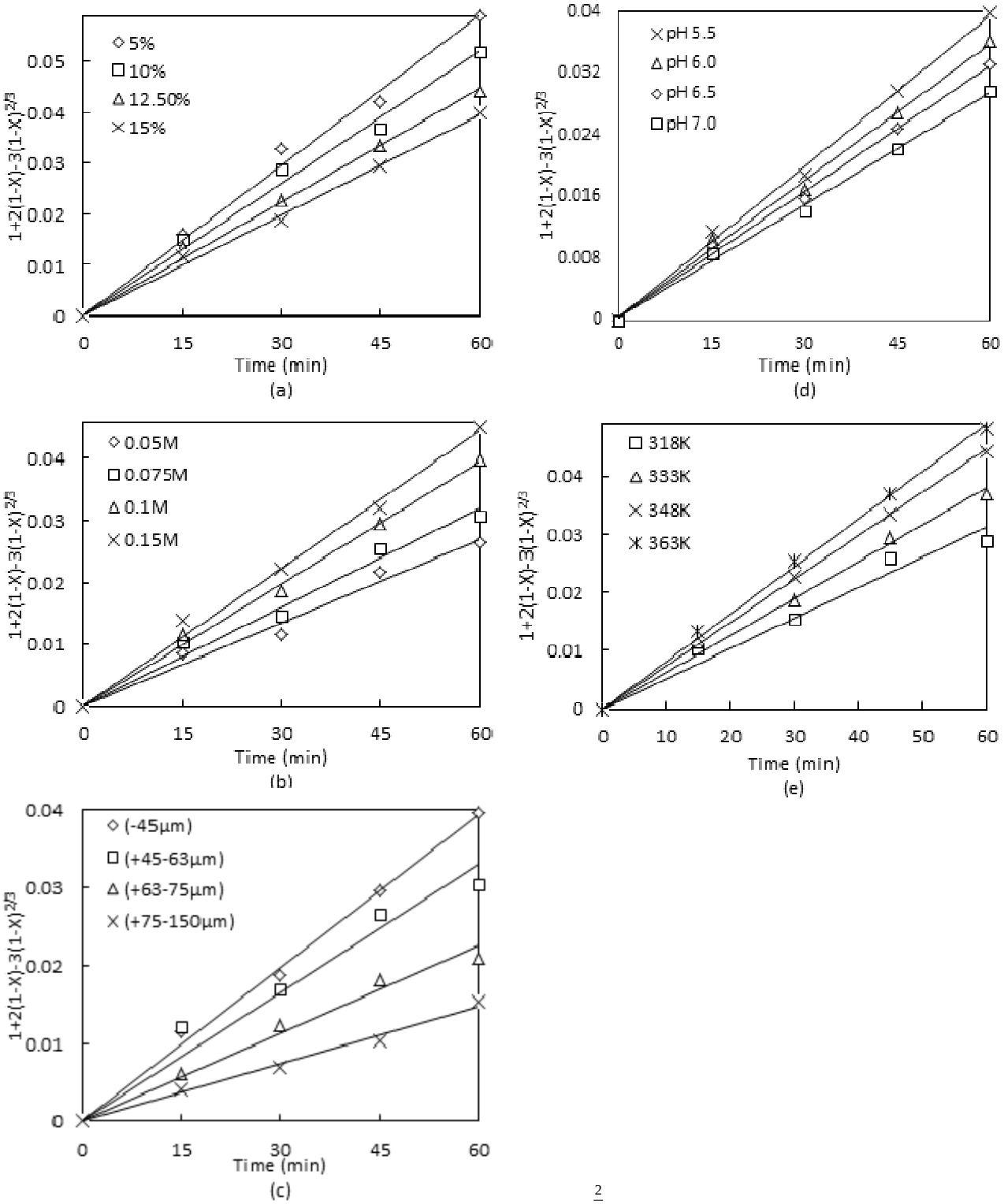

Figure 5. Linear relationship showing variation of $1+2(1-X)-3(1-X)^{\frac{2}{3}}$ *with the reaction time for different solid-to-liquid ratio (a), acid concentration (b), particle size (c), pH (d) and temperature (e).*

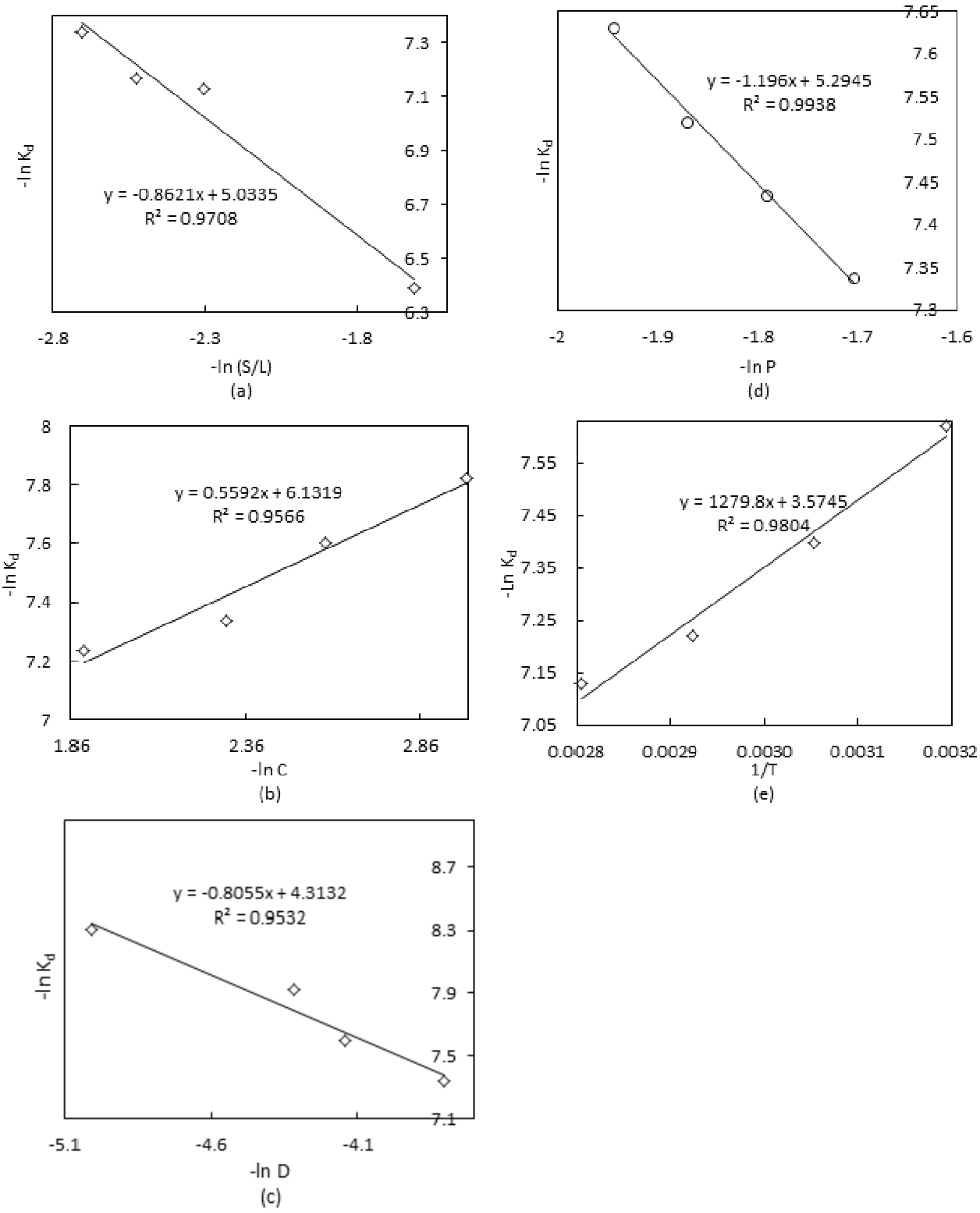

Figure 6. Variation of -ln K_d with -ln S/L (a), -ln C (b), -ln D (c), -ln P (d) and 1/T (e) (Arrhenius plot).

The activation energy for the process was determined to be 10.64 kJ/mol.

Nomenclature

FGD – Flue gas desulphurization
b – Stoichiometric coefficient
K_l – Mass transfer coefficient (m min^{-1})
C_A – Bulk concentration (mol cm^{-3})
ρ_B – Sorbent molar density (kg mol m^{-3})
R_o – Initial particle radius (m)
t – Reaction time (min)
D_e – Product layer effective diffusion coefficient (m^2 min^{-1})
K_d – Product layer reaction rate constant (min^{-1})
K_s – Surface reaction rate constant (m min^{-1})
E_a – Activation energy (kJ mol^{-1})
R – Universal gas constant (kJ mol^{-1} K^{-1})
T – Temperature (K)
C – Acid concentration (mol dm^{-3})
S/L – Solid-to-liquid ratio (g ml^{-1})
D – Particle size (μm)
P – pH

REFERENCES

[1] S. Mishra, S. Langwenya, B. Mamba, M. Balakrishnan, Phys. Chem. Earth **35** (2010) 811-814

[2] J. Temuujin, R. Williams, A. Van Riessen, J. Mater. Process. Technol. **209** (2009) 5276-5280

[3] T. Bakharev, Cement Concrete Res. **35** (2005) 1224--1232

[4] J. Swanepoel, C. Strydom, Appl. Geochem. **17** (2002) 1143-1148

[5] F. Goodarzi, Fuel **85** (2006)1418-1427

[6] H. Song, J. Park, Environ. Technol. **22** (2001) 1001-1006

[7] D. Ogenga, Z. Siagi, M. Onyango, M. Mbarawa, Front. Chem. Sci. Eng. **3** (2009) 46-51

[8] R. Lin, S. Shih, Powder Technol. **131** (2003) 212-222

[9] W. Jozewicz, G.T. Rochelle, Environ. Prog. **5** (1986) 219--224

[10] S. Kashiwakura, H. Ohno, Y. Kumagai, H. Kubo, K. Matsubae, T. Nagasaka, Chemosphere **85** (2011) 598-602

[11] H. Brouwers, R. Van Eijk, J. Mater. Sci. **37** (2002) 2129--2141

[12] H.S. Pietersen, A.L. Fraay, J.M. Bijen, MRS Online Proc. Libr. **89** (1989)

[13] H. Tanaka, A. Fujii, Adv. Powder Technol. **20** (2009) 473--479

[14] L. Koech, R. Everson, H. Neomagus, H. Rutto, in Proceedings of International Conference on Chemical, Mining and Metallurgical Engineering, Johannesburg, South Africa, 2013, p. 233

[15] S.D. Rocha, M.B. Mansur, V.S. Ciminelli, J. Chem. Technol. Biotechnol. **79** (2004) 816-821

[16] G. Dube, P. Osifo, H. Rutto, Clean Technol. Environ. Policy **16** (2014) 891-900

[17] N. Karatepe, A. Mericboyu, S. Küçükbayrak, Energy Sources **20** (1998) 505-511

[18] K.T. Lee, S. Bhatia, A.R. Mohamed, J. Mater. Cycles Waste Manage. **7** (2005) 16-23

[19] H. Hadjar, B. Hamdi, M. Jaber, J. Brendlé, Z. Kessaissia, H. Balard, J. Donnet, Microporous Mesoporous Mater. **107** (2008) 219-226

[20] P. Adamiec, J. Benezet, A. Benhassaine, Particuology **6** (2008) 93-98

[21] M. Criado, A. Fernández-Jiménez, A. Palomo, Microporous Mesoporous Mater. **106** (2007)180-191

[22] K. Thiruppathi, S. Barathan, N. Anandhan, G. Sivakumar, Appl. Phys. Res. **59** (2009) 1-9

[23] S.M. Nyale, O.O. Babajide, G.D. Birch, N. Böke, L.F. Petrik, Procedia Environ. Sci. **18** (2013) 722-730

[24] Z. Sarbak, M. Kramer-Wachowiak, Powder Technol. **123** (2002) 53-58

[25] E. van der Merwe, C. Strydom, J. Therm. Anal. Calorim. **84** (2006) 467-471

[26] W. Hsu, M. Lin, J. Hsu, Int. J. Chem. Biol. Eng. **2** (2009) 4-8

[27] N. Demirkıran, Braz. J. Chem. Eng. **141** (2008) 180-186

[28] O. Levenspiel, Chemical Reaction Engineering, 3rd ed., John Wiley and Sons, New York, 1972, p. 583

[29] P. Maina, M. Mbarawa, Energy Fuels **25** (2011) 2028--2038

[30] R.H. Limo, C. Enweremadu, Chem. Ind. Chem. Eng. Q.. **17** (2011) 459-468

[31] Z.I. Zafar, Chem. Eng. J. **141** (2008) 233-241

[32] J. Zhao, Y. Li, K. Han, S. Niu, C. Lu, J. Chem. Eng. Jpn. **46** (2013) 827-832.

LAWRENCE KOECH[1]
RAY EVERSON[2]
HEIN NEOMAGUS[2]
HILARY RUTTO[1]

[1]Department of Chemical Engineering, Vanderbijlpark Campus, Vaal University Of Technology, Vanderbijlpark, South Africa
[2]Department of Chemical and Minerals Engineering, Potchefstroom Campus, North West University, Potchefstroom, South Africa

NAUČNI RAD

KINETIKA RASTVARANJA LETEĆEG PEPELA JUŽNOAFRIČKOG UGLJA I RAZVIJANJE POLUEMPIRIJSKOG MODELA ZA PREDVIĐANJE RASTVARANJA

Mokra desulfurizacija dimnog gasa (FGD) predstavlja presudnu tehnologiju, koja se može koristiti za smanjenje emisije sumpor-dioksida u elektranama na ugalj. Rastvaranje letećeg pepela uglja u adipinskoj kiselini je praćeno promenom koncentracije kiseline (0,05-0,15 M), veličine čestice (45-150 mm), pH (5.5-7.0), temperature (318-363 K) i odnosa čvrsto-tečno (5-15 mas.%.) tokom perioda od 60 min, što je ključni korak u mokrom postupku. Karakterizacija sorbenta je urađena pomoću X-fluoroscentne analize (XRF), X-difrakcionae analize (XRD), Furrier infracrvene analize (FTIR), skening elektronske mikroskopije (SEM) i Brunauer-Emmett-Teller metode (BET) za specifičnu površinu. BET rezultati pokazuju povećanje specifične površine, dok SEM analiza ukazuje na to da je nakon rastvaranja formirana porozna struktura. Eksperimentalni podaci su analizirani korišćenjem modela neizreagovanog jezgra i pokazalo se da je stupanj koji određuje brzinu reakcije upravo difuzija kroz sloj produkta. Izračunato je da aktivaciona energija za proces iznosi 10,64 kJ/mol.

Ključne reči: desulfurizacija dimnog gasa, leteći pepeo, rastvaranje, model neizreagovanog jezgra, aktivaciona energija.